Estimation of Diffusion Coefficients for Multiple Penetrant/Polyolefin Systems Based on Sorption Data

Rita F. Alves, Timothy Frederick Llewellyn Mckenna

Estimation of Diffusion Coefficients for Multiple Penetrant/Polyolefin Systems Based on Sorption Data

Rita Ferreira Alves, Timothy F.L. McKenna*

Université de Lyon, CNRS, CPE-Lyon, UCB Lyon-1, Chimie Catalyse Polymères et Procédés (C2P2), 43 Blvd du 11 Novembre 1918, 69616 Villeurbanne Cedex, France

*timothy.mckenna@univ-lyon1.fr

Abstract

The binary and ternary diffusion coefficients for gas/polymer systems can be estimated from solubility data and an equation of state to the free volume of penetrant/polymer systems. The system free volume can be calculated by the Sanchez Lacombe equation-of-state (SL-EoS), eliminating the need for viscoelastic data in determination of free volume parameters. Furthermore, this approach accounts for polymer swelling. The model gives reliable predictions for both binary and ternary systems of alkanes and alkenes in polyolefins.

Key Words: Polymer; diffusion; solubility; equation of state; swelling

1. Introduction

A detailed understanding of diffusion processes is clearly essential for many different types of production processes in general, and polymerization processes in particular. Diffusion of gases and liquids can be the limiting step during chemical reactions in multiphase systems, and during purification and degassing operations as well. In the specific case of olefin polymerization processes, estimation of the diffusion of reactants and other components is further complicated by the highly non-ideal nature of the thermodynamics [1], the impact of physical properties such as crystallinity that govern the sorption and transport processes in materials such as polyolefins [2], and a significant lack of available data concerning sorption and diffusion, especially under industrially pertinent conditions. It would therefore be useful if one could estimate parameters such as the diffusion coefficient of mixture of gases through polymers in a simple, straight forward manner

As an example of what we mean by the impact of non-ideal thermodynamics, let us consider a ternary system made up of two solutes (components 1 and 2) and a semi-crystalline polymer such as polyethylene or polypropylene (component 3). The 2 solutes are soluble in the amorphous portion of the polymer and can diffuse through that phase if there is a gradient of chemical potential. Otherwise it is assumed that the crystalline phase remains impermeable to the penetrants [3]. In an industrial environment, it is not uncommon to find non-reactive solutes, often referred as Induced Condensing Agents (ICA), can be present as liquids, or more generally as part of the vapour phase in most of the reactor. These compounds are used to enhance heat removal, but do not influence the reactivity of the catalyst. If the light solute is ethylene [4–7] (or propylene [8]) and the heavier one an ICA such as pentane or hexane, adding the ICA can leading to a doubling of the observed rate of reaction. Furthermore, Alizadeh *et* al. [9] showed that simply accounting for the increased solubility of ethylene due to the ICA is not sufficient if one wishes to model the entire reaction. At long times, the cosolubility effect (modelled using the Sanchez-Lacombe Equation of State – SL-EoS) adequately accounted for the increase in the reaction rate that was observed experimentally. However, during the first few minutes of the polymerization, the authors showed using a free volume-based model that accounts for the presence of the ICA for the effective diffusivity of ethylene in the amorphous phase of the polymer led to a better fit of the reactor mode. These modelling results validate a discussion in an earlier paper by Floyd and Ray [10] who reached two important conclusions: (i) the diffusion coefficient of vapors depends significantly on

their concentration in the amorphous polymer phase; (ii) the presence of ICA or other vapors that might swell the polymer will lead to an increase of the diffusion coefficient.

These (and many other) results highlight the need to develop a predictive model of the diffusion behavior of monomer in the amorphous polymer phase when ICA is present. One of the most widely used approaches used to this objective relies on the free volume theory which was developed then extensively modified by Fujita [11] and Vrentas and Duda [12,13]. The approach developed by Vrentas and Duda [12–16] seems to be quite successful for the prediction of diffusion coefficients of penetrants in polymers [17], and this approach has been widely investigated to improve its accuracy and applicability to multiple cases.

The free volume can be thought of as the unoccupied space between molecules in solution. For molecular migration to take place in the amorphous phase of a polyolefin, two prerequisites must be satisfied: (i) there must be a hole (or free volume) space of sufficient size adjacent to a penetrant molecule; (ii) that same molecule must have enough energy to overcome intermolecular interactions to jump into the hole. For a polymer above its glass transition temperature, the polymer chains can adjust their segment motion by thermal vibration and the available free volume usually becomes the predominant factor for the rate of diffusion. From these notions, Duda *et al.* [15] developed the well-known expressions for the self-diffusion coefficient of the penetrant, D_1, and mutual-diffusion coefficient, D, for binary systems. These expressions are given by equations (1) and (2).

$$D_1 = D_0 \cdot \exp\left(\frac{E_a}{R \cdot T}\right) \cdot \exp\left(\frac{\omega_1 \cdot \hat{V}_1^* + \omega_3 \cdot \xi_{1,3} \cdot \hat{V}_3^*}{V_{FH}/\gamma}\right) \quad (1)$$

$$D = D_1 \cdot (1 - \emptyset_1)^2 \cdot (1 - 2 \cdot \chi \cdot \emptyset_1) \quad (2)$$

In equation (1) D_0 is a pre-exponential factor that is only dependent on the penetrant, E_a is the diffusion activation energy, ω_i is the mass fraction of the *ith* component, $\hat{V}_i^*$ is the critical hole free volume required for the *ith* component to make a jump, $\xi_{1,3}$ is the ratio of critical molar volumes, V_{FH} is the free volume and γ is an overlap factor that accounts for the same free volume being available for both species. In equation (2) $\emptyset_1$ is the volume fraction of component 1 and χ is the Flory-Huggins interaction parameter, which denotes the intermolecular interactions between polymer and penetrant [18]. The self-diffusivity of the molecules in a lattice occurs without the presence of a gradient of chemical potential. In this

case, no matter which direction the penetrant jumps to, the dispensed energy is the same, as there is no chemical potential gradient. The mutual diffusion, however, occurs in the presence of a driving force which is a gradient of chemical potential, often approximated by a concentration gradient.

If one examines equation (1), it becomes clear that the self-diffusivity is related to the ratio of the occupied volume and the total free volume: the numerator accounts for the volume that is already occupied by the jumping units. The $\xi_{1,3}$ factor mitigates the difference in size of the solute and polymer jumping units, thus allowing for a better evaluation of the contribution of each species for the occupied volume [19]. The denominator is the total available free volume in the system.

In the traditional Vrentas-Duda approach to the Free Volume Theory, the hole free volume (V_{FH}) is estimated by (13) for the binary case:

$$V_{FH}/\gamma = \omega_1 \cdot \frac{K_{1,1}}{\gamma} \cdot \left(K_{3,1} - T_{g,1} + T\right) + \omega_2 \cdot \frac{K_{1,3}}{\gamma} \cdot \left(K_{3,3} - T_{g,3} + T\right) \quad (3)$$

Where $K_{1,1}$ and $K_{3,1}$ are penetrant free volume parameters, $K_{1,3}$ and $K_{3,3}$ are polymer free volume parameters and $T_{g,i}$ is the *ith* component glass transition temperature. As suggested by Duda [18], these parameters (and D_0 in equation (1)) are obtained by regression of the viscosity and specific volume data as a function of the temperature for the pure penetrant and polymer. Hong [20] reported this data for several systems and compared the diffusion coefficients from the Vrentas-Duda theory regressed with the viscosity-temperature data and the experimental diffusion coefficients. The results showed that the Vrentas-Duda approach closely replicates the experimental diffusion behavior [20]. However, one key point to underline at this juncture is that this approach requires experimental data which may not always be easily found.

Expression (2) is a result of equation 4 [18]:

$$D = D_1 \cdot \frac{\rho_1 \cdot \bar{v}_3 \cdot \rho_3}{R \cdot T} \cdot \left(\frac{\partial \mu_1}{\partial \rho_1}\right) \quad (4)$$

Where ρ_i is the density of the *ith* component, $\bar{v}_3$ is the partial specific volume of the polymer. To obtain eq. (2), the Flory-Huggins model in equation (5) can be used to calculate the penetrant chemical potential, which is then introduced into eq. (4) to calculate $\left(\frac{\partial \mu_1}{\partial \rho_1}\right)$ [21].

$$\mu_1 = \mu_1^0 + R \cdot T \cdot \left(\ln(1 - \emptyset_3) + \chi \cdot {\emptyset_3}^2 + \emptyset_3\right) \quad (5)$$

Kulkarni *et al*. [22] used Fujita's approach [11] to model the binary diffusion and solubility coefficients for CO_2, CH_4, C_2H_4, and C_3H_8 in polyethylene at temperatures ranging from 5 to 35^oC and gas pressures up to 40 atm., and presented correlations for the free-volume parameters. They found that these parameters were mainly dependent on size, shape and kinetic velocity of the penetrant molecules. The authors were then able to relate these parameters to the Lennard-Jones size parameter and molecular weight, which proved to be useful, as these are easy to get parameters. However, this approach falls short when polymer swelling is significant.

Vrentas and Duda [14] and Wesselingh and Bollen [23] extended the Free volume Theory for self-diffusion in multicomponent mixtures (penetrant(1)-penetrant(2)-polymer(3)). Vrentas and Duda [14] found that for the chosen systems the self-diffusion coefficients could be accurately modelled from the binary data (i.e. penetrant(1)-polymer(3) and penetrant(2)-polymer(3)) studies. This conclusion was corroborated by Schabel *et al.* [24] for the ternary system. However, their approach is limited to the self-diffusion coefficient and by the available experimental data/parameters. When these are not readily available, they can be very hard to obtain.

In another study by Vrentas and Duda [25] the authors relate the mutual diffusion with self-diffusion in ternary systems, building on a friction-based theory and analyzing the limit of small concentrations. Their approach has been extended by a number of other studies, including that of Alsoy and Duda [26], who proposed four alternative approximations for the mutual and cross-diffusion coefficients. These ranged from considering mutual diffusion equal to self-diffusion to more complicated expressions where the diffusion coefficients are dependent on a thermodynamic term while the friction factors are kept constant. Price and Romdhane [27] reviewed and generalized the existent friction-based theories for self- and mutual diffusion coefficients. Vanag *et al.* [28] have explored the subject of ternary reaction-diffusion systems and demonstrated the importance of cross-diffusion. Arya *et al.* performed a sensitivity analysis of the free volume theory parameters and concluded that their model predictions were highly sensitive to the penetrant(s)-polymer jumping unit ratios($\xi_{i,j}$). Cancelas e*t al.*[29] studied the diffusivity of ethylene, propylene and ethylene-propylene mixtures in isotactic polypropylene (iPP) and found that the effective diffusivity of ethylene-propylene mixtures is lower than that of either of the individual gases.

More related to the interest of this study, several authors have studied the impact of polymer swelling and have shown that it can be significant when considering a wide penetrant concentration range [30–32]. All authors concluded that polymer swelling will affect the diffusion behavior, with Duda *et al.* [30] pinpointing that for a swelling degree higher than 3%, the modelling approach needs to account for a moving boundary condition at the polymer-gas interface on the calculation of effective diffusion. Furthermore, Kanellopoulos *et al.* [31] show that polymer swelling increases the diffusion rate. However, no studies were found in the literature that showed the impact of polymer swelling in the ternary systems.

Equation-of-state models, such as the Sanchez-Lacombe (SL-EoS) [33] are often applied to polymeric systems, as they can be used to accurately predict polymer-penetrant behavior, while retaining a relative mathematical simplicity. Two studies by Wang *et al.* [19][34] estimate the polymer Free Volume Theory parameters using an Equation-of-state approach, and obtained good predictions of the binary diffusion coefficients. In their first work [19] the authors used the S-S Hole theory [35], while in their most recent work they used SL-EoS [34]. In both cases the EoS were used to estimate the contribution of the polymer phase to the system free volume. This leaves the estimation of the penetrant contribution to the traditional Vrentas and Duda approach, which is limited by the available data for the penetrant phase free volume parameters and doesn't accounting for swelling effects. Additionally Wang *et al.* limited their work to binary systems.

The present work is based on an approach similar to that of Wang *et al* [19][34], but is different in it's application as we will show that it is useful to combine a thermodynamic Equation of State model (here SL-EoS) with the free volume theory. This allows us to extend the model to ternary (or in principle higher order) systems, and to calculate the free volume parameters for both polymer and gas-phase from solubility data using the EoS. This means that the impact of swelling, co-penetrant and anti-penetrant effects can be included in the prediction of diffusion coefficients. The developed model is structured in such a way that all parameters can be calculated using solubility data and a pre-exponential factor that depends only on the nature of the penetrant.

2. Model Development

In this work, a modified approach to the free volume theory for the calculation of binary and ternary diffusion coefficients is combined with the Sanchez-Lacombe Equation of State. This

will eliminate the need for viscoelastic data in determination of free volume parameters, which may be hard to obtain. Furthermore, this approach can account for polymer swelling which has been demonstrated to impact diffusion behavior. Although experimental solubility data is still required to fit SL-EoS, this type of data is more readily available (especially for binary systems), or measurable than the methods proposed by Duda *et al.*[18].

Note that the free volume theory and the SL-EoS are only applicable to the amorphous polymer phase. However, the approach presented here relies on solubility data for a given system, so when one optimises the interaction parameters that actually means that we account for the impact of crystallinity on the solubility, and thus the method is applicable to semi-crystalline polymers. As discussed in section 1 the diffusion of penetrant(s) is negligible in the crystalline phase of the polymer [10] . We can therefore introduce the crystallinity weight fraction in the self-diffusion expressions [22].

2.1 Sanchez-Lacombe Equation-of-State

According to the Sanchez-Lacombe Equation-of-State lattice-fluid model (SL-EoS) [36] the polymer chains are treated as a set of connected beads on a lattice. The presence of empty sites or holes is permitted in the lattice, but since the lattice size is fixed, the changes in volume are governed by changes in the number of holes [37].

For a polymer liquid, the SL-EoS in terms of reduced variable is given by:

$$\bar{\rho}^2 + \bar{P} + \bar{T} \cdot \left[\ln(1-\bar{\rho}) + \left(1 - \frac{1}{r}\right) \cdot \bar{\rho}\right] = 0 \tag{6}$$

Where $\bar{\rho}$, $\bar{P}$, $\bar{T}$ are the reduced density, pressure and temperature, and are defined as:

$$\bar{T} = T/T^* \,,\ \bar{P} = P/P^*,\ \bar{\rho} = \rho/\rho^* \tag{7}$$

Where T^*, P^* and ρ^* are, respectively, the characteristic temperature, pressure and close-packed mass density, which completely characterize a pure fluid. r is the number of sites a molecule occupies in the lattice. In principle, any thermodynamic property can be utilized to determine these parameters, but saturated pressure data is often employed for its wide availability [37]. Several authors have published tables where these molecular parameters are made available [36]. This model requires as well an interaction parameter, k_{ij}, which is dependent on the solute(s)-polymer system used and temperature [37]. One way to obtain this

interaction parameter is to fit the SL-EoS to solubility data, which is widely found for binary systems and found for some ternary systems.

The SL model is an Equation of State, meaning equation (6) includes the total thermodynamic description of the polymer-penetrant(s) system. This means that all thermodynamic properties, such as isobaric thermal expansion coefficient or chemical potential, follow from the standard thermodynamic formulae and can be easily derived from expression (6). Details regarding the SL-EoS parameters and solution strategy can be found elsewhere [38,39].

2.2 Binary System

Analyzing the molar diffusion flux given by Fick's Law:

$$j_i = -D \cdot \nabla C_i \tag{8}$$

Here the gradient of molar fraction (∇C_i) of the diffusing component i is assumed to approximate the driving force for the diffusion process that is the chemical potential. The proportionality coefficient, D, is the diffusivity in the amorphous phase of the polymer, and that can in principle be found using the free volume theory as described above. The diffusivity of a penetrant(1) in the polymer(3) can be found by relating the self-diffusivity and the mutual-diffusivity. The self-diffusivity is given by equation (1). The mutual diffusivity coefficient is given by equation (4). The parameter $\left(\frac{\partial \mu_1}{\partial \rho_1}\right)$ in this equation is now estimated using the SL-EoS, shown in equation 9:

$$\begin{aligned}\mu_1 = {} & \mathrm{R\,T}\,[\ln(\emptyset_1) + 1 - \emptyset_1] + \\ & r_1\left\{-\bar{\rho}\left[\frac{2}{\alpha\emptyset_1+\beta}\left((M'\emptyset_1 + N') - \left(\frac{A\cdot\emptyset_1{}^2+B\cdot\emptyset_1+C}{\alpha\emptyset_1+\beta}\right)(M''\emptyset_1 + N'')\right) + \left(\frac{A\emptyset_1{}^2+B\emptyset_1+C}{\alpha\emptyset_1+\beta}\right)\right]\right. \\ & \left.\frac{R\cdot T}{\bar{\rho}}\left[(1-\bar{\rho})\ln(1-\bar{\rho}) + \frac{\bar{\rho}}{r_1}\ln(\bar{\rho})\right] + \frac{P}{\bar{\rho}}(2(M''\emptyset_1 + N'') - \alpha\emptyset_1 + \beta)\right\}\end{aligned} \tag{9}$$

$\emptyset_1$ closed-packed volume fraction of solute molecules in the polymer phase and $\bar{\rho}$ is the polymer phase reduced density. $\alpha, \beta, A, B, C, M', N', M'', N''$ are parameters which can be calculated based on v_1^*, v_2^*, v_{1-2}^* (closed packed molar volume of a site 1, 2 and 1-2) and $\varepsilon_1^*, \varepsilon_2^*, \varepsilon_{1-2}^*$ (1, 2, 1-2 site-site interaction energy, where $\varepsilon_{1-2}^* = \sqrt{\varepsilon_1^* \varepsilon_2^*}\,(1 - k_{12})$). k_{12} is the aforementioned interaction parameter [38,39].

2.3 Ternary Case

When exploring the ternary case of diffusion, one must extend Fick's law to the multicomponent case:

$$j_1 = -\sum_{j=1}^{n-1} D_{ij} \cdot \nabla C_i \tag{10}$$

In a mixture of n components, (n-1) independent diffusion fluxes exist. Fick's law needs to be extended and generalized in order to take into account the interactions between fluxes and concentration gradients of different diffusing components. The flux of diffusing component *i* now depends upon the concentration gradients of other components in the mixture. Fick's description of multicomponent diffusion involves a matrix of (n-1)^2 diffusion coefficients, which generally is not symmetric. The matrix of diffusion coefficients consists of the main and the cross diffusivities. Main diffusivity D_{ii} connects the flux of a component with its own concentration gradient, while cross diffusivities D_{ij} connect the flux of the i^{th} component with the concentration gradients of other components [28]. In this work the cross-diffusion coefficients will be considered zero. It has been shown elsewhere [28] that cross-diffusion is only important when a chemical reaction takes place, which is outside the scope of this work.

Following the approach of Vrentas and Duda [14], the self-diffusivity of penetrant(1) and penetrant(2) in the polymer(3) is given by equations (11) and (12).

$$D_1 = D_{0,1} \cdot \exp\left(\frac{E_a}{R \cdot T}\right) \cdot \exp\left(\frac{\omega_1 \cdot \hat{V}_1^* + \omega_2 \cdot \hat{V}_2^* \cdot \xi_{1,2} + \omega_3 \cdot \xi_{1,3} \cdot V_3^*}{V_{FH}/\gamma}\right) \tag{11}$$

$$D_2 = D_{0,2} \cdot \exp\left(\frac{E_a}{R \cdot T}\right) \cdot \exp\left(\frac{\omega_1 \cdot \hat{V}_1^* \cdot \xi_{2,1} + \omega_2 \cdot \hat{V}_2^* + \omega_3 \cdot \xi_{2,3} \cdot V_3^*}{V_{FH}/\gamma}\right) \tag{12}$$

Subsequent to the friction-based approach, one can relate the self-diffusion and friction factors to arrive at the mutual diffusion coefficient. However, there are many more friction factors than self-diffusion coefficients – this means that relating the self- and mutual diffusion coefficients requires additional assumptions.

In the case where solute concentrations tend to zero (a reasonable approximation, for instance in gas phase olefin polymerizations), Vrentas *et al.* [25] considered that the cross-diffusion coefficients go to zero, and the resultant main term diffusion coefficient is given by eqs. (13) and (14).

$$D_{11} = (1 - \rho_1 \cdot \bar{v}_1) \cdot \rho_1 \cdot D_1 \left(\frac{1}{RT} \cdot \frac{\partial \mu_1}{\partial \rho_1}\right) - \rho_2 \cdot \bar{v}_2 \cdot \rho_1 \cdot D_2 \left(\frac{1}{RT} \cdot \frac{\partial \mu_2}{\partial \rho_1}\right) \tag{13}$$

$$D_{22} = (1 - \rho_2 \cdot \bar{v}_2) \cdot \rho_2 \cdot D_2 \left(\frac{1}{RT} \cdot \frac{\partial \mu_2}{\partial \rho_2}\right) - \rho_1 \cdot \bar{v}_1 \cdot \rho_2 \cdot D_1 \left(\frac{1}{RT} \cdot \frac{\partial \mu_1}{\partial \rho_2}\right) \quad (14)$$

1

2 2.4 Parameter estimation

3 The estimation of the critical hole free volume ($\hat{V}_i^*$), ratio of penetrant and polymer jumping
4 units ($\xi_{i,j}$) and partial specific volume ($\bar{v}_i$), required for the presented model equations, can be
5 found in the supporting information. The procedure to estimate the hole free volume and a
6 discussion on the pre-exponential factor and activation energy are presented below.

7 2.4.1 Hole free volume (V_{FH})

8 The free volume is given by equation (15) [19].

$$V_{FH}/\gamma = V \cdot f_{FV} \quad (15)$$

9 In which V is the specific volume ($m^3.kg^{-1}$), and f_{FV} is the free volume fraction.

10 According to Ferry [40], the free volume fraction for the polymer phase at atmospheric
11 pressure and polymer glass transition temperature, $f_{FV}\left(T_{g,2}, P_0\right)$, is 0.0025. The fractional
12 free volume at the temperature and pressure of interest can be obtained by considering the
13 isobaric and isothermal processes:

$$f(T, \mathrm{P}) = f\left(T_{g,2}, P_0\right) + \int_{T_{g,2}}^{T} \alpha_f\big|_{P_0} dT - \int_{P_0}^{P} \beta_f\big|_{T} dP \quad (16)$$

14 Where α_f and β_f are, respectively, the isobaric thermal expansion and isothermal
15 compressibility factors.

16 For polymeric liquids (and in a semi-crystalline polymer, we assume the amorphous phase
17 behaves like a liquid), α_f is given by [40]:

$$\alpha_f = \alpha_l - \alpha_0 \quad (17)$$

18 Where α_0 is the thermal expansion coefficient of the occupied volume, and α_l is the thermal
19 expansion coefficient of the total volume of the polymer phase. Since there is no way to attain
20 the value of α_0, in this work it will be considered that $\alpha_l \gg \alpha_0$, as the thermal expansion for a
21 polymer is much greater than that of the occupied volume [19,40].

22 The value of β_f can be expressed by:

$$\beta_f = \beta_l - \beta_g \quad (18)$$

In which β_l is the compressibility factor above T_g, and β_g is the compressibility factor just below T_g. Since the SL-EoS is applied for polymers in thermodynamic equilibrium, only the β_l can be estimated. β_g is set to be equal to half of β_l [19,40].

Substituting in equation (16), the volume fraction of free volume at temperature and pressure of interest is then given by equation (18):

$$f(T,\mathrm{P}) = 0.025 + \int_{T_{g,2}}^{T} \alpha_l|_{P_0} dT - \frac{1}{2}\int_{P_0}^{P} \beta_l|_T dP \quad (19)$$

Here, α_l and β_l are given by the appropriate differentiation of equation (6) [19]:

$$\alpha_l = \frac{1}{V}\frac{\partial V}{\partial T}\Big|_P = -\frac{\partial ln(\bar{\rho})}{\partial T}\Big|_P = \frac{1 + \bar{P}/\bar{\rho}^2}{T \cdot \left[\frac{\bar{T}}{\bar{\rho}} \cdot \left(\frac{1}{(1/\bar{\rho}+1)} + \frac{1}{r}\right) + 2\right]} \quad (20)$$

$$\beta_l = -\frac{1}{V}\frac{\partial V}{\partial P}\Big|_T = \frac{\partial \ln(\bar{\rho})}{\partial P}\Big|_T = \frac{\bar{P}/\bar{\rho}^2}{P \cdot \left[\frac{\bar{T}}{\bar{\rho}} \cdot \left(\frac{1}{(1/\bar{\rho}+1)} + \frac{1}{r}\right) + 2\right]} \quad (21)$$

The group of Wang *et al*. [34] applied the above definition to the polymer phase, as they treated the penetrant and polymer phases independently. This leaves the calculation of penetrant contribution to the free volume to be calculated by the traditional Vrentas and Duda method. In this work, the above definitions of α_f and β_f are applied to the polymer phase that is considered to be swollen by the presence of penetrant, thus calculating the thermal expansion and compressibility factors for the mixture of gas plus polymer. This will strip the model of the need to know the free volume parameters for the penetrant. However, solubility data is required in order to calculate the SL-EoS interaction parameters, k_{ij}. While solubility for multicomponent systems representative of olefin polymerizations are rare, they can be found at least as easily as the free volume parameters, if not more easily.

2.4.2 Pre-exponential factor (D_0)

The pre-exponential factor is often overlooked as "just a constant" that appears in self-diffusion expressions. However, when analyzing these expressions we can see that it represents the penetrant self-diffusion for the limit of infinite dilution ($\omega_1 \approx 0$). Therefore, this parameter is of import when employing the FVT for diffusion in polymeric systems, as an accurate estimation of this parameter is essential for good model predictions.

An important term related to the pre-exponential factor is the activation energy (E_a), which represents the energy per mole that a molecule requires to overcome the attractive forces binding it to its neighbors. Other than estimating the activation energy based on experimental data, no other methods were found that linked any penetrant properties to its activation energy. Even so, Vrentas and Duda [18,41] argue that for the sake of better regression fits, its best to consider $E_a = 0$. When this is the case, the pre-exponential factor is noted as $D_{0,1}$, to symbolize that this value was adjusted to experimental data without an estimation of the activation energy. This approximation imposes certain limitations, since not including the activation energy is the same as dismissing the effects of temperature in D_0. This may influence of the predictive abilities of the model when considering large temperature intervals, although for temperatures that vary only over a small range, the model shows good agreement with experimental data [18,26,31,42].

Vrentas and Duda [18,41] also discuss the hypothesis that the pre-exponential factor is solely a property of the penetrant. With this in mind, an effort was made to correlate the pre-exponential factor to penetrant properties. The Lennard-Jones size parameter has been used by Kulkarni [22] to estimate Fujita's version of pre-exponential factors for gaseous penetrants in polyethylene. Their correlation can only be applied to small molecules, smaller than *n*-hexane (which no longer fits in with their data). Nevertheless, this suggested that a size parameter might be a well suited contender to correlate the pre-exponential factor. The figure bellow shows the relation between the molecular diameter and a pre-exponential factor ($D_{0,1}$). The experimental $D_{0,1}$ values presented below were obtain all from the same study by Duda *et al*. [18]. The data was fitted with a decaying exponential equation. It is worth noting that the list of penetrants presented by Duda *et al* includes an array of different families of molecules, ranging from alkanes, alkenes, ketones and organic halogen compounds.

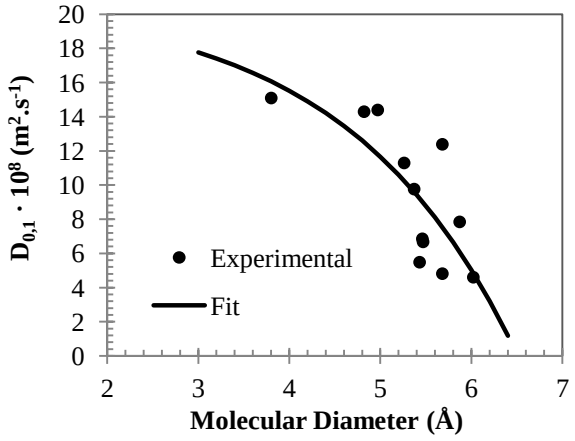

Figure 1. Pre-exponential factor, $D_{0,1}$, varying with molecular diameter. Experimental data obtained from [18]**.**

Figure 1 shows that there is an apparent trend where $D_{0,1}$ decreases as a function of the molecular diameter. If all the data is included, a decaying exponential function of $D_{0,1}$ as a function of molecular diameter appears to roughly follow the evolution of the experimentally measured values. However, as discussed above, a precise estimate of the pre-exponential factor is essential for good model predictions, and deviations between the exponential fit for $D_{0,1}$ and experimental values are too large to provide the required precision. Therefore, in this work the values D_0, $D_{0,1}$, and E_a used were found in the literature for the relevant systems. This conclusion, combined with the definition of D_0 and E_a leaves open the discussion if these are indeed penetrant only parameters.

2.5 Solubility data and SL-EoS model fitting

The SL-EoS interaction parameter (k_{ij}) were found by fitting the model to experimental solubility data of pure and mixtures of gaseous olefins and alkanes in various polymers found in the open literature. Table 1 shows the characteristic SL parameters for the considered components in this work.

Table 1. Molecular characteristic parameters for Sanchez-Lacombe EoS.

Component	P* (bar)	T* (K)	ρ^* (kg. m^{-3})	Ref
Methane	2500	152	500	[43]

Ethylene	3395	283	680	[44]
Propylene	3788	345.4	755	[29]
n-Pentane	3060	445	755	[39]
n-Hexane	2979	476	775	[39]
LDPE	4399	655	900	[45]
LLDPE	4360	653	903	[39]
iPP	3007	690.6	885.6	[29]

The systems and temperatures for which relevant solubility data was found and corresponding developed k_{ij} correlations with temperature are shown in Table 2.

Table 2. Modelled solubilities in this study.

Comp 1	Comp 2	Polymer	T (^{o}C)	k_{ij}	Ref
Propylene	-	iPP	50; 70; 85	k_{12}= -0.0076·T(K) + 0.27	[29]
Ethylene	-	iPP	50; 70; 85	k_{12}= -0.00028·T(K) + 0.082	[29]
Ethylene	Propylene	iPP	50; 70; 85	k_{13}= -0.00011·T(K) + 0.021	[29]
				k_{23}= -0.00061·T(K) + 0.21	
n-Hexane	-	PE	70; 80; 85; 90	k_{23}= 0.0014·T(K)-0.48	[46]
Ethylene	-	PE	60; 70; 80; 90	k_{12}= -0.0011·T(K) + 0.38	[46]
Ethylene	*n*-hexane	PE	70; 80; 90	k_{13}=0.000030·T(K) + 0.0054[a]	[46]
				k_{23}=0.00050·T(K) - 0.15 [a]	
n-Pentane	-	PE	70;85;90	k_{12}=0.00086·T(K) - 0.27	[46]
Ethylene	*n*-Pentane	PE	70;80;90	k_{13}=0.000045·T(K)+0.00044[b]	[46]
				k_{23}=0.00056·T(K) - 0.15 [b]	
Methane	-	LDPE	40;80	k_{12}= -0.0013·T(K) + 0.26	[47]

[a] k_{ij} adjusted keeping *n*-hexane partial pressure between 0.6 and 0.7 bar.
[b] k_{ij} adjusted keeping *n*-pentane partial pressure between 1.6 and 1.8 bar.

3. Results and Discussion

3.1 Model Validation

Table 3 shows the required model parameters that have not been estimated: the pre-exponential factors (D_0 or $D_{0,1}$) and the diffusion activation energy.

Table 3. Pure component diffusion model parameters.

Component	T_g (K)	$D_{0,1}$ ($m^2.s^{-1}$) [a]	D_0 ($m^2.s^{-1}$) [b]	E_a ($J.mol^{-1}$)	Ref
Methane	-	$1.51x10^{-9}$	-	0	[48]
Ethylene	-	-	2.96×10^{-6}	8786	[49]
Propylene	-	-	7.65×10^{-6}	15899	[49]
iso-Pentane	-	6.68×10^{-8}	-	0	[50]
n-Hexane	-	7.85×10^{-8}	-	0	[18]
LDPE	148	-	-	-	[51]
LLDPE	193	-	-	-	[31]
iPP	253	-	-	-	[49]

[a] Pre-exponential factor adjusted to experimental data while keeping E_a=0
[b] Pre-exponential factor and E_a adjusted to experimental data

3.1.1 Binary Case

The model validation was carried out on a range of different polymers and penetrants.

Figure 2 shows the mutual diffusion of *n*-pentane in high density polyethylene (HDPE) polymers. It can be seen that the model is able to correctly describe the diffusion behavior of the system and predict the impact of changing temperature, all with a difference between experimental data and model predictions of less than 9%.

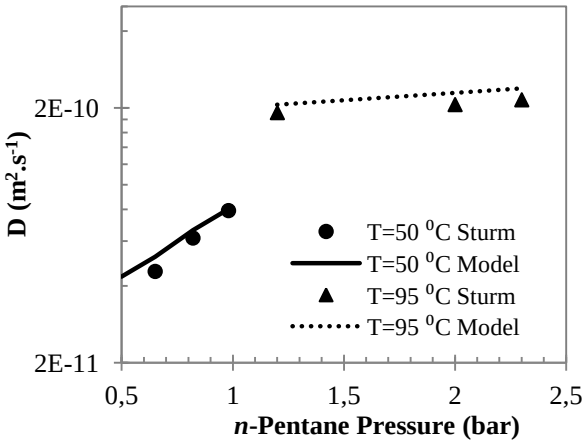

Figure 2. Diffusivity of *n*-pentane in HDPE at 50 °C and 95 °C varying with total pressure. Experimental obtained by Sturm [50]**.**

Flaconneche *et al.* [47] studied the solubility and diffusion of methane in LDPE for pressures ranging from 40 to 100 bar at 40 °C and 80 °C. The results in Figure 3 show that the model is

also able to correctly predict their experimental diffusivity values of methane for higher pressure systems. Additionally, it should be pointed out that the D_0 parameter used in these calculations was obtained by another author [48], and not fitted to this particular set of data.

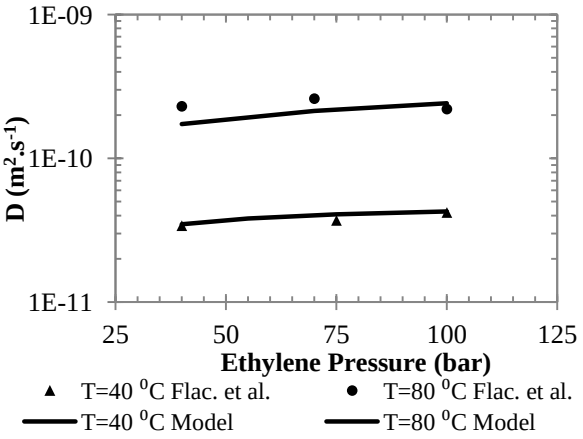

Figure 3. Diffusivity of methane in LDPE at 40 °C and 80 °C varying with total pressure. Experimental obtained by Flaconneche *et al.* [47]**.**

The binary model was also validated with a single set of parameters using two independent data sets of the diffusivity of propylene and ethylene in iPP obtained by Cancelas *et al*. [29] and Gonzalez *et al.* [49].

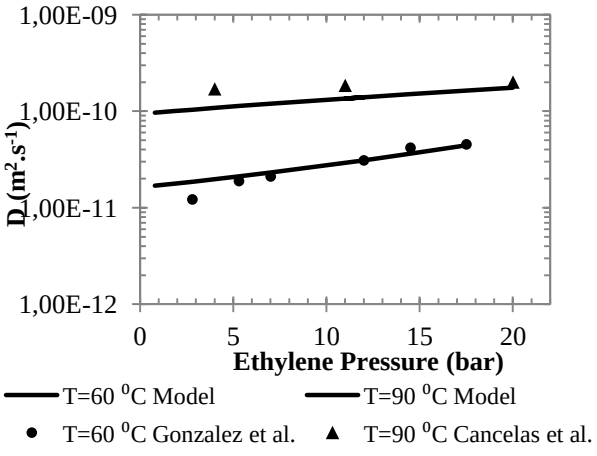

Figure 4. Diffusivity of ethylene in iPP at 60 °C and 90 °C varying with total pressure. Experimental at 60 °C obtained by Gonzalez *et al.* [49] **and 90 °C by Cancelas *et al.*** [29]**.**

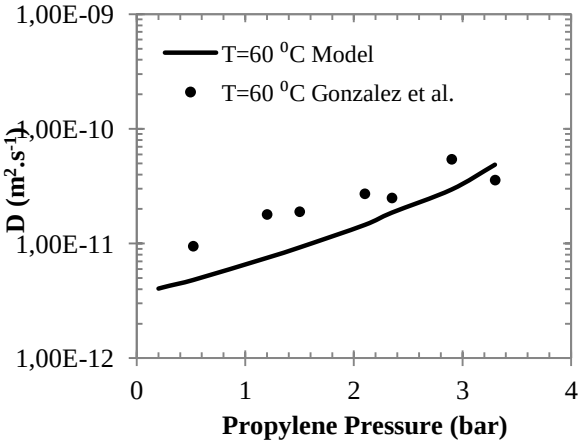

Figure 5. Diffusivity of propylene in iPP at 60 °C varying with total pressure. Experimental data obtained by Gonzalez *et al.* [49].

Figures 4 and 5 show that the model predicts the mutual diffusion behavior for the chosen systems. For ethylene and propylene diffusion in iPP, the model captures the diffusion trend, even when there are changes in temperature.

The table below shows the results obtained Cancelas *et al*. [29] and how they compare to the model results.

Table 4. Comparison of the results obtained by Cancelas et al. [29] **and this model and corresponding difference between model prediction and reported experimental data (Δ).**

T (^{0}C)	Pressure (bar)	Average Diffusion·10^{-11} ($m^2.s^{-1}$)					
		Propylene			Ethylene		
		Experimental	Model	Δ (%)	Experimental	Model	Δ (%)
50	4	3.0	4.8	60	3.7	2.6	29
50	11	3.5	8.3	132	4.5	4.0	12
90	4	12.0	6.5	46	17.0	9.6	43
90	11	17.0	19.3	13	18.5	14.1	24
90	20	17.0	46.8	175	20.0	21.6	8

In this table, it is clear that the numerical values of the model do not agree nearly as well with the data obtained by Cancelas *et al*. [29] for the propylene/iPP and ethylene/iPP systems. It should be noted that the experimental values for the diffusion of propylene in iPP at 90°C do not follow the expected trend, where we would expect that the measured value of the

diffusivity would be a stronger function of pressure. Furthermore, the model fits Gonzalez's data set very well for propylene, so it is possible that the experimental values of reference are incorrect, and not the model predictions.

To check the validity of the model, we used the characteristic length scale provided by Cancelas *et al.* [29] for their sorption experiments, and our value of the predicted mutual diffusivity value in Crank's [52] analytical expression for diffusion in a sphere:

$$\frac{M(t)}{M_{eq}} = 1 - \frac{6}{\pi^2}\sum_{n=1}^{\infty}\frac{1}{n^2}exp\left\{-Dn^2\pi^2\frac{t}{r^2}\right\} \quad (22)$$

where $M(t)$ is the mass sorbed at a given time t, M_{eq} is the total mass sorbed at equilibrium, r is the characteristic length scale for diffusion, and D is the diffusivity of the sorbant. The obtained result compared with the experimental sorption curve and with the best diffusion fit for the experimental curve, obtained by minimizing the residuals. The results for ethylene sorption in iPP at 90 ^{0}C and 4 bar are shown in Table 5 and Figure 6, where it can be seen that the predicted value of diffusivity fits the data reasonably well.

Table 5. Comparison of the diffusion results for ethylene in iPP at 90 ^{0}C and 4 bar. Data obtained by Cancelas.

Diffusion $\cdot 10^{-11}$ ($m^2.s^{-1}$)		
Best Fit	Model	Δ (%)
11.5	9.6	20

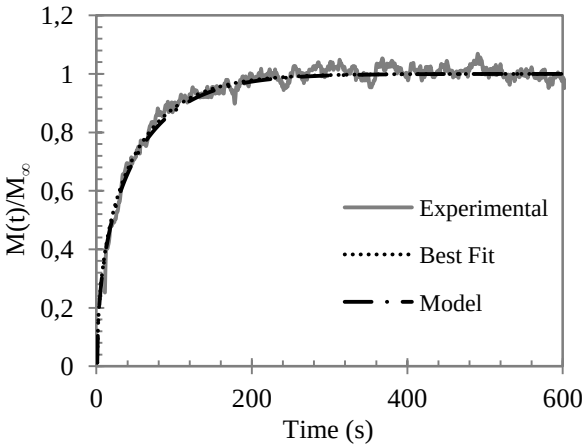

Figure 6. Comparison of the sorption curves for ethylene in iPP at 90 ^{0}C and 4 bar. Data obtained by Cancelas, this work (model) and the best fit to the sorption curve.

3.1.2 Ternary Case

The ternary model predictions of overall diffusivity of a mixture of ethylene and propylene diffusion in iPP, were compared to the same values also estimated in the work of Cancelas *et al*. [29]. The experiment results only show the total diffusion for the mixture of ethylene and propylene, whilst the developed model accounts for the mutual diffusion of the species separately. To obtain an equivalent diffusion coefficient to the one attained experimentally, "partial" sorption curves were obtained using the modelled mutual diffusion coefficients, and corresponding solubility values. These curves (shown as the broken lines in figure below) were then added, realizing the total sorption curve (full line in figure below), which represents the results obtained by [24]. The analytical solution of the diffusion equation for spheres developed by Crank [52] was once again used to fit a diffusion coefficient to the newly-modelled curve. Table 6 shows the summary of the diffusion coefficients obtained for a gaseous equimolar mixture of ethylene and propylene diffusing in iPP.

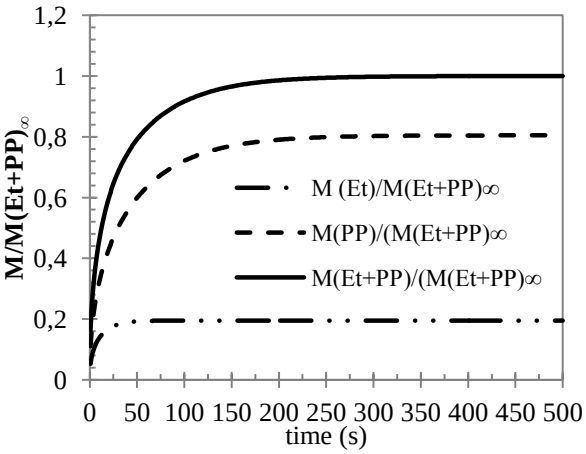

Figure 7. Sorption curves obtained using the analytical diffusion solution and the modelled diffusion results.

The analytical solution of the diffusion equation (22) was once again employed for two different temperatures and pressures, in order to validate the model. Experimental values of best fit average diffusivities obtained from unpublished data provided by Cancelas Sanz, and obtained as described in reference [29] are shown in Table 6, and selected curves shown in Figure 8. The results presented in Table 6 and Figure 8 show that the ternary model predictions are quite close to the best fit of the experimental data, and that they predict the sorption data quite well.

Table 6. Comparison of the best fit diffusion results with model predictions for mixtures of ethylene and propylene in iPP, for different temperatures, pressures and molar fraction in the gas phase.

T (^{0}C)	Pressure (bar)	% (molar) Ethylene	% (molar) Propylene	Average Diffusion $\cdot 10^{-11}$ ($m^2.s^{-1}$)		
				Best Fit	Model	Δ (%)
50	4	50	50	1.7	1.2	40
50	11	25	75	3.7	4.8	23
50	11	50	50	2.4	3.1	22
50	11	75	25	1.4	1.8	23
50	20	50	50	3.2	5.3	40
90	11	50	50	9.0	11.2	20
90	20	50	50	23.6	20.8	14

It can be seen from Table 6 that the diffusion coefficient of the gas mixture decreases as molar fraction of ethylene increases. This is to be expected, as a smaller propylene fraction results in less available free volume, which influences for the diffusion rates. It is also shown that the model predicts the trends of diffusion coefficients for the chosen system in all the available temperature and pressure ranges and while varying gas phase composition. However, for some experimental data sets (mainly at 50 ^{0}C and 4 and 11 bar), the model captures the order of magnitude of the reported experimental results, but fails to predict the diffusion coefficient accurately. To further examine the implications of this, figure 8 shows the experimental sorption curves for two temperatures and pressures while comparing them to the best fit and the diffusion coefficient predicted by the model.

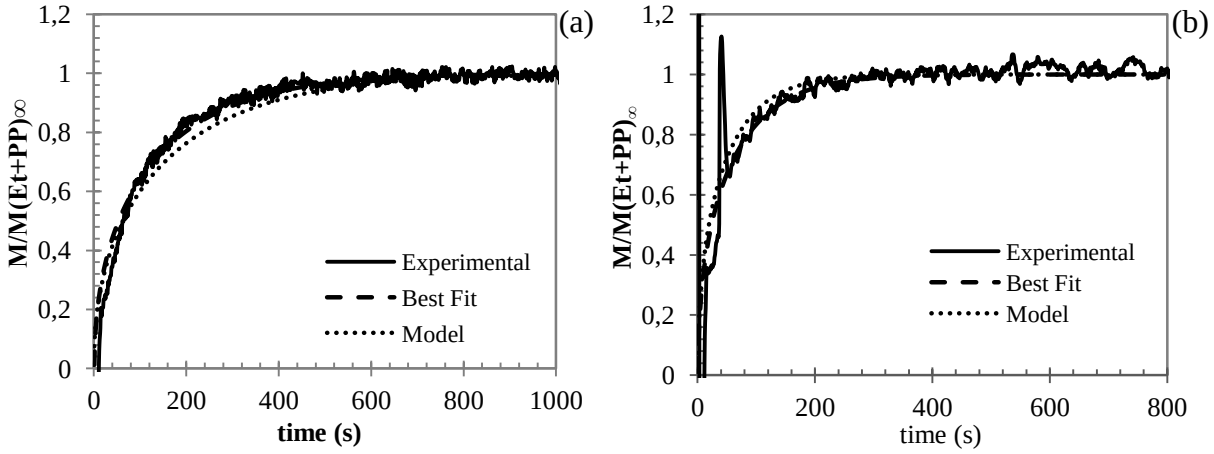

Figure 8. Comparison of the sorption curves for an equimolar mixture of ethylene and propylene in iPP at (a) 50 ^{0}C and 4 bar; (b) 90 ^{0}C and 11 bar. Data obtained by Cancelas.

Figure 8 (a) is especially important, as this predicted model value set is one that exhibits one of the biggest differences to the best fit to experimental data (about 40%). Still, it is shown that modelled value describes the sorption curve. In figure (b) it is possible to see that with a difference of 20% between best fit to experimental data and predicted diffusion coefficients the sorption curves are almost completely overlapped.

Coupling the extensive validation completed for the binary case with the results presented in this section, the model is considered reasonably valid.

3.2 Free Volume Results

Figure 9 shows a comparison of the free volume as given by Vrentas and Duda (equation (3)) and the free volume obtained in this work by the method described above. The results show good agreement, further validating the model and assumptions made in section 3.3.

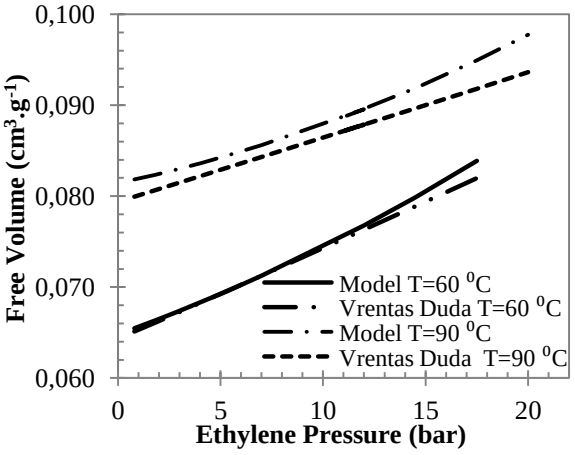

Figure 9. Comparison of the free volume calculated by Vrentas and Duda'a approach [49] **and this work for the Ethylene/iPP system at 60^{0}C.**

As the pressure is increased it can be observed that the two models start to diverge slightly. This can be explained by the fact that Vrentas and Duda use mixture parameters that do not take into account polymer swelling, while model proposed here does. Figure 10 shows that when the swelling is not accounted for, the free volume estimation using the method described in section 2.4.1., takes a linear shape, closer to the results obtained by Vrentas and Duda. In this figure one can also see the corresponding predicted degree of swelling for each pressure. It then becomes clear that a higher swelling degree corresponds to more available free volume.

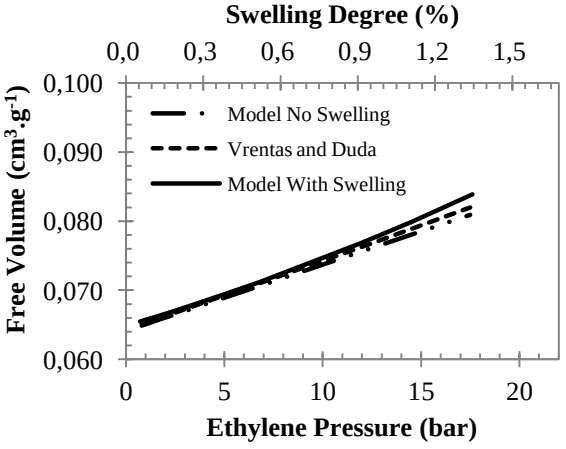

Figure 10. Comparison of free volume estimation by Vrentas and Duda approach [49]**, this work not accounting for polymer swelling and this work accounting for polymer swelling in function of total pressure and swelling degree. Ethylene/iPP system at 60^{0}C.**

Comparing the free volume obtained for binary and ternary systems, the results were as expected. As seen in Figure 11, the ternary free volume sits between the two binary free volumes. The same Figure also shows the comparison between the free volume calculated by

this model and estimated by Vrentas and Duda's approach. The same trend is observed as in the binary systems, where the curve takes a different shape for higher pressures, due to the polymer swelling. It is also possible to observe that the total ternary free volume takes a similar shape to the free volume for the *n*-hexane/LLDPE system, suggesting that this parameter is controlled by the heavier component.

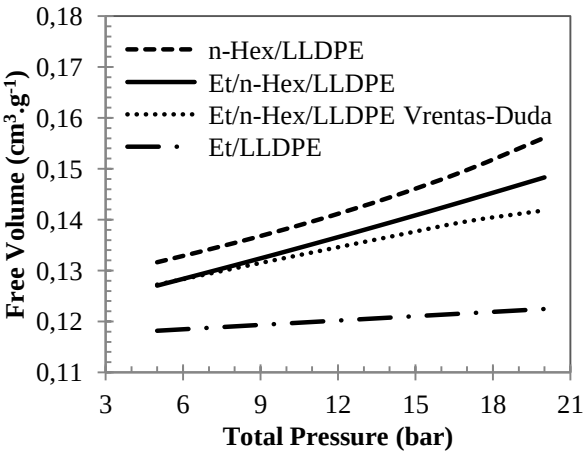

Figure 11. Free volume for Ethylene, *n*-hexane and a mixture of both in LLDPE varying mixture total pressure (calculated by this model and by Vrentas and Duda approach [9]**) at 70^{0}C. Pressure of *n*-hexane varying between 0.4-0.8 bar.**

3.3 Diffusion Results

Figure 10 shows the mutual diffusion of ethylene, *n*-pentane and *n*-hexane in LLDPE varying with the mass fraction. The results obtained are as expected, where the diffusion coefficient increases with temperature and mass fraction.

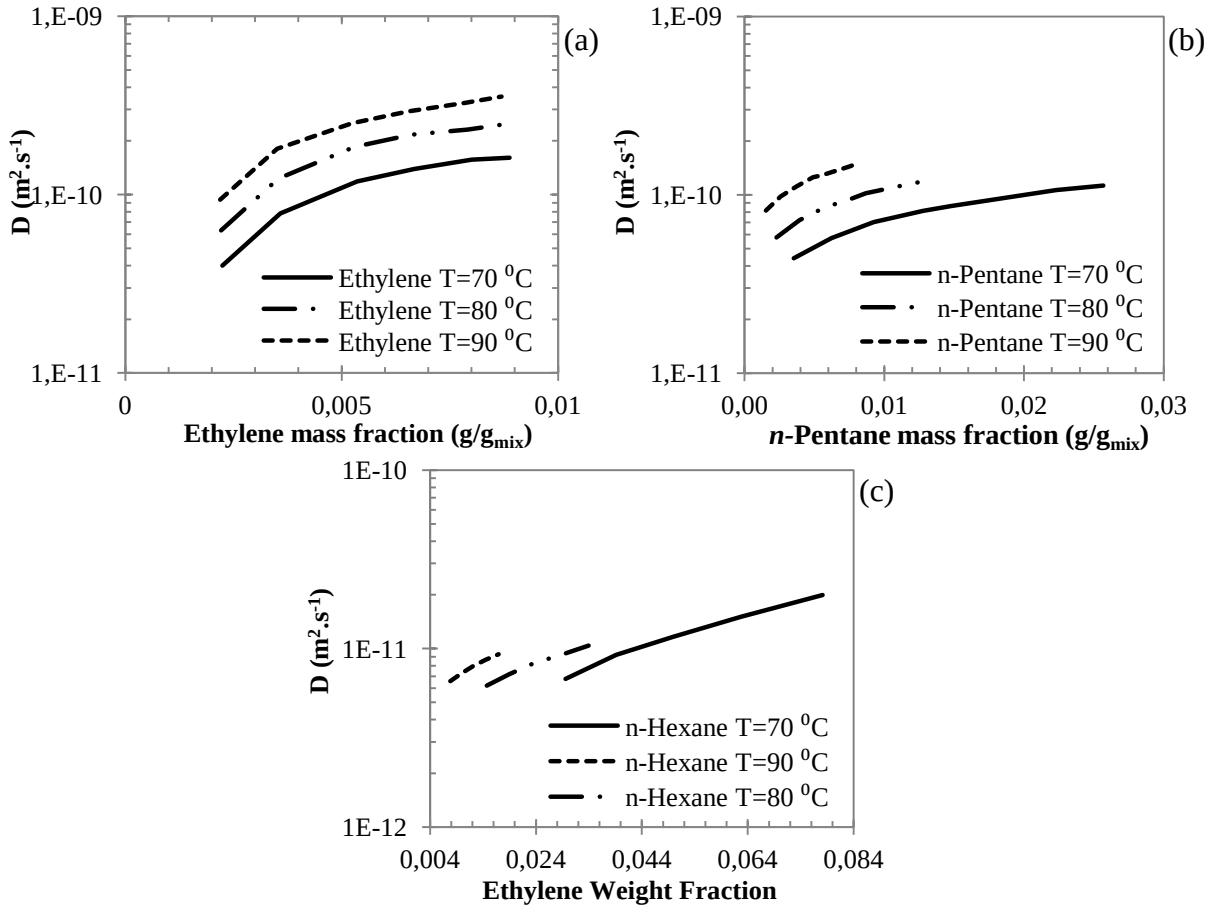

Figure 12. Mutual diffusion of ethylene (a), *n*-pentane (b) and *n*-hexane (c) in LLDPE at 70, 80 and 90 °C.

To evaluate the effects of ICA in the diffusion of ethylene, two ternary systems were studied: ethylene/*n*-hexane/LLDPE and ethylene/*n*-pentane/LLDPE.

In the first set of simulations, the total pressure was varied while the molar fraction of the gas phase remained fixed.

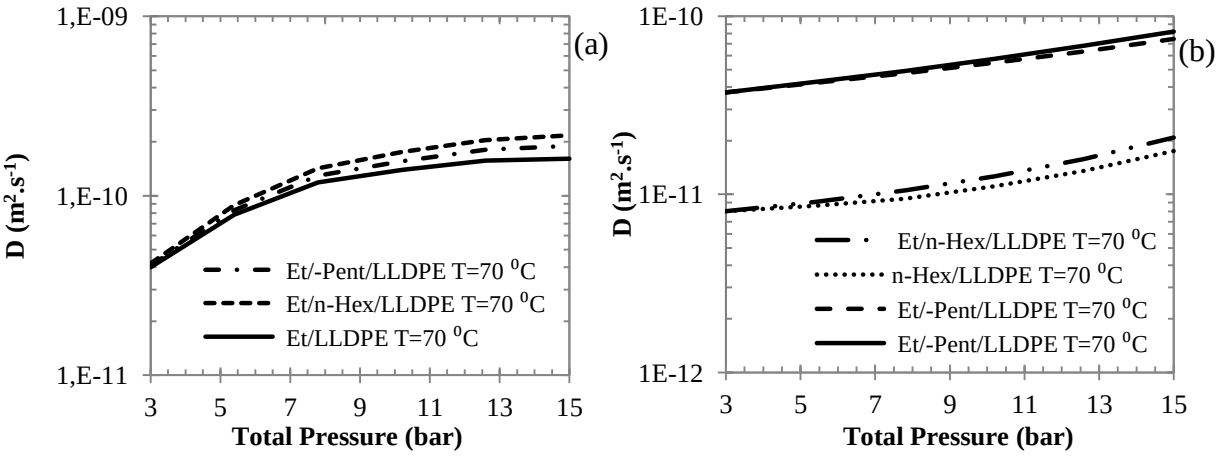

Figure 13. Mutual diffusion coefficient of Ethylene (a) and n-hexane or n-Pentane (b) in LLDPE in binary and ternary systems with n-hexane (5% molar in the gas phase) or n-pentane (15% molar in the gas phase) at 70^{0}C.

Figure 13 shows that the ethylene diffusion in the presence on an ICA is increased when compared to the binary. This is due to two main effects that the ICA will have on the system: (i) co-solubility effects – the presence of an ICA increases the solubility of ethylene in the amorphous phase; (ii) the ICA will swell the polymer, increasing free volume allowing for faster ethylene diffusion, as discussed in section 4.2. By adding 5% n-hexane to the mixture we can observe a 30% increase in the ethylene diffusion coefficient, while adding 15% molar of n-pentane to the mixture leads to a 22% increase. It can be observed that the diffusion of both ICA's increase when we move from the binary to the ternary system, which may not be an expected result because of the anti-penetrant effect – while the ethylene solubility is increased due to the presence of an ICA, the ICA solubility decreases due to the presence of ethylene. However, what is observed is that there is more free volume in the ternary system than compared to the binary system. This shows that the available free volume is controls diffusion rates.

Considering the system ethylene/*n*-hexane/LLDPE, and keeping the total pressure constant (at 12 bar), increasing the molar fraction of n-hexane present in the mixture (from 0 to 5%) at 70^{0}C we obtain the following results in terms of relative diffusion:

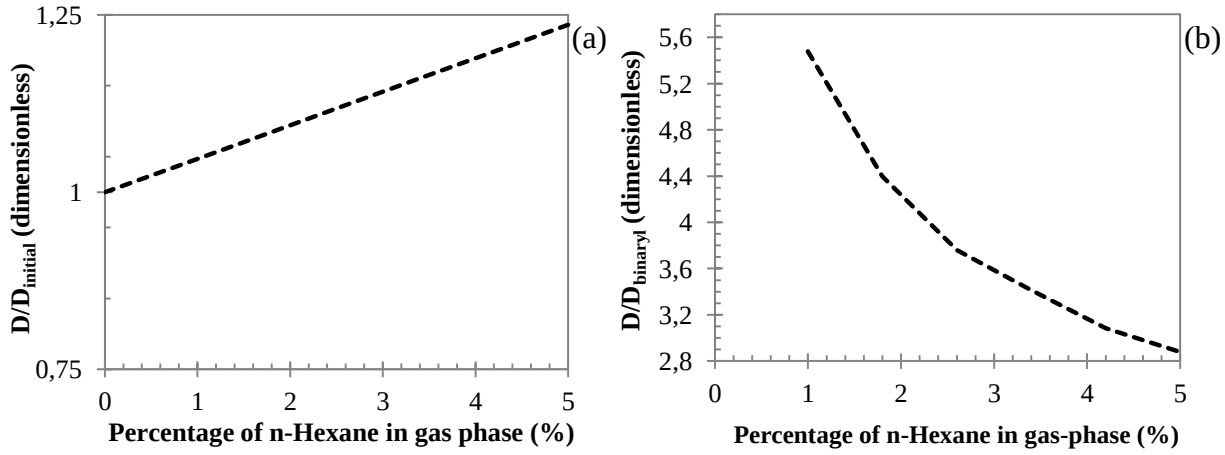

Figure 14. The enhancement magnitude in the mutual diffusion of ethylene (a) and *n*-hexane (b) at 12 bar varying with the n-hexane molar fraction in the gas-phase at 70^{0}C. *n*-hexane diffusion is normalized with the corresponding binary system at the same partial pressures.

Figure 14 shows that increasing up to 5% the molar percentage of *n*-hexane, increases the diffusion of ethylene by a factor of about 1.24. In the n-hexane case, it can be observed that the even though the enhancement diminishes with the increase of *n*-hexane (due to the anti-penetrant effect), the diffusion of *n*-hexane in the ternary case is always faster than the binary case. This is expected, as the presence of ethylene increases the available free volume, which is especially important at the beginning when the mass fraction of *n*-hexane in the polymer is lower.

Considering a fixed monomer pressure, Figure 14 shows the effects of adding ICA into a process on the diffusivity.

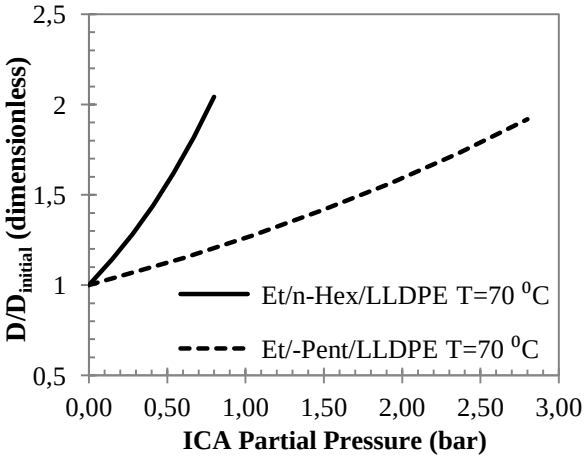

Figure 15. Effect of adding *n*-hexane or *n*-pentane as ICA on the diffusion of ethylene in LLDPE at 70 ^{0}C. Partial pressure of ethylene is kept constant at 7 bar.

From the results shown in figure 15 it's possible to compare the effects of both ICA in the diffusion of ethylene. If one considers the effect of adding 0.8 bar of *n*-hexane, it's possible to see an increase of 51%, while adding the same amount of *n*-pentane leads to only an increase of 17%. This difference is expected, as the bigger size of n-hexane compared to n-pentane leads to more noticeable co-solubility effects and swelling - which translates in more available free volume.

4. Conclusions

A mathematical model has been developed for the prediction of binary and ternary diffusion coefficients based on the free volume theory. The model relies on solubility data of the gas (or gases) in the polymer phase and on a pre-exponential factor, which may be solute dependent only. The model has been validated and shows good agreement with the available experimental data. The free volume calculated was compared with Vrentas and Duda's approach and also showed good agreement.

For the binary case, the results show that the diffusion coefficient increases with temperature and pressure, as expected and in agreement with other studies.

For the ternary case, it is shown that the co-solubility effect of ICA has an effect in the diffusion of monomer, as it increases the free volume and monomer's solubility. It was observed that the diffusivity of ICA also increases from the binary to the ternary system, regardless of the anti-penetrant effect. This revealed that the available free volume the controlling factor the diffusion rate.

The coupling of the SL-EoS with the free volume also proved to be advantageous when working with semi-crystalline polymers: Using solubility data obtained for semi-crystalline polymer to SL-EoS implies that the diffusion model accounts for amorphous areas of the polymer that are not accessible to the penetrants due to crystallinity constraints.

This method for calculating diffusion coefficients could easily extended to other polymer systems or classes of molecules. The original free volume theory was developed in a generalized matter, meaning that the main limitations in this work arise from using SL-EoS. However, this approach can be implemented with any other thermodynamic model, making this work applicable to a variety of systems.

Acknowledgements.

The authors are grateful to ExxonMobil Chemical Company for financial support of this work.

1

2

3

4

5

5. References

[1] S.K. Nath, A. Brian J. Banaszak, J.J. de Pablo, Simulation of Ternary Mixtures of Ethylene, 1-Hexene, and Polyethylene, (2001). doi:10.1021/MA002197L.

[2] A.B. Michaels, R.W. Haussleix, Elastic factors controlling sorption and transport properties of polyethylene, J. Polym. Sci. Part C Polym. Symp. 10 (2007) 61–86. doi:10.1002/polc.5070100107.

[3] A.S. Michaels, H.J. Bixler, Solubility of gases in polyethylene, J. Polym. Sci. 50 (1961) 393–412. doi:10.1002/pol.1961.1205015411.

[4] A. Alizadeh, M. Namkajorn, E. Somsook, T.F.L. McKenna, Condensed Mode Cooling for Ethylene Polymerization: Part I. The Effect of Different Induced Condensing Agents on Polymerization Rate, Macromol. Chem. Phys. 216 (2015) 903–913.

[5] M. Namkajorn, A. Alizadeh, E. Somsook, T.F.L. McKenna, Condensed Mode Cooling for Ethylene Polymerisation : The Influence of Inert Condensing Agent on the Polymerisation Rate, Macromol. Chem. Phys. 215 (2014) 873–878.

[6] A. Alizadeh, M. Namkajorn, E. Somsook, T.F.L. McKenna, Condensed Mode Cooling for Ethylene Polymerization: Part II. From Cosolubility to Comonomer and Hydrogen Effects, Macromol. Chem. Phys. 216 (2015) 985–995.

[7] R. Alves, M.A. Bashir, T.F.L. McKenna, Modeling Condensed Mode Cooling for Ethylene Polymerization: Part II. Impact of Induced Condensing Agents on Ethylene Polymerization in an FBR Operating in Super-Dry Mode, Ind. Eng. Chem. Res. 56 (2017) 13582–13593. doi:10.1021/acs.iecr.7b02963.

[8] A.R. Martins, A.J. Cancelas, T.F.L. McKenna, A Study of the Gas Phase Polymerization of Propylene: The Impact of Catalyst Treatment, Injection Conditions and the Presence of Alkanes on Polymerization and Polymer Properties, Macromol. React. Eng. 11 (2017) 1600011. doi:10.1002/mren.201600011.

[9] A. Alizadeh, F. Sharif, M. Ebrahimi, T.F.L. McKenna, Modeling Condensed Mode Operation for Ethylene Polymerization: Part III. Mass and Heat Transfer, Ind. Eng. Chem. Res. 57 (2018) 6097–6114. doi:10.1021/acs.iecr.8b00330.

[10] S. Floyd, K.Y. Choi, T.W. Taylor, W.H. Ray, Polymerization of Olefins through

Heterogeneous Catalysis III. Polymer Particle Modelling with an Analysis of Intraparticle Heat and Mass Transfer Effects, J. Appl. Polym. Sci. 32 (1986) 2935–2960.

[11] H. Fujita, Diffusion in polymer-diluent systems, Fortschritte Der Hochpolym. 3 (1961) 1–47. doi:10.1007/BF02189382.

[12] J.S. Vrentas, J.L. Duda, Diffusion in polymer—solvent systems. I. Reexamination of the free-volume theory, J. Polym. Sci. Polym. Phys. Ed. 15 (1977) 403–416. doi:10.1002/pol.1977.180150302.

[13] J.S. Vrentas, J.L. Duda, Diffusion in polymer–solvent systems. II. A predictive theory for the dependence of diffusion coefficients on temperature, concentration, and molecular weight, J. Polym. Sci. Polym. Phys. Ed. 15 (1977) 417–439. doi:10.1002/pol.1977.180150303.

[14] J.S. Vrentas, J.L. Duda, H.-C. Ling, Self-diffusion in polymer-solvent-solvent systems, J. Polym. Sci. Polym. Phys. Ed. 22 (1984) 459–469. doi:10.1002/pol.1984.180220308.

[15] J.L. Duda, J.S. Vrentas, S.T. Ju, H.T. Liu, Prediction of diffusion coefficients for polymer-solvent systems, AIChE J. 28 (1982) 279–285. doi:10.1002/aic.690280217.

[16] J.S. Vrentas, C.M. Vrentas, A new equation relating self-diffusion and mutual diffusion coefficients in polymer-solvent systems, Macromolecules. 26 (1993) 6129–6131. doi:10.1021/ma00074a040.

[17] J.S. Vrentas, J.L. Duda, A.-C. Hou, Evaluation of theories for diffusion in polymer–solvent systems, J. Polym. Sci. Polym. Phys. Ed. 23 (1985) 2469–2475. doi:10.1002/pol.1985.180231205.

[18] J.M. Zielinski, J.L. Duda, Predicting polymer/solvent diffusion coefficients using free-volume theory, AIChE J. 38 (1992) 405–415. doi:10.1002/aic.690380309.

[19] H.-L. Lv, B.-G. Wang, Prediction of solvent diffusion coefficient in amorphous polymers based on an equation-of-state, J. Polym. Sci. Part B Polym. Phys. 44 (2006) 1000–1009. doi:10.1002/polb.20750.

[20] S.-U. Hong, Prediction of Polymer/Solvent Diffusion Behavior Using Free-Volume Theory, Ind. Eng. Chem. Res. 34 (1995) 2536–2544. doi:10.1021/ie00046a040.

[21] P.J. Flory, Principles of Polymer Chemistry, Cornell University Press, New York, 1953.

[22] S.S. Kulkarni, S.A. Stern, The diffusion of CO2, CH4, C2H4, and C3H8 in polyethylene at elevated pressures, J. Polym. Sci. Polym. Phys. Ed. 21 (1983) 441–465. doi:10.1002/pol.1983.180210310.

[23] J.A. Wesselingh, A.M. Bollen, Multicomponent diffusivities from the Free Volume Theory, Trans IChemE. 75 (1997) 590–602. doi:10.1205/026387697524119.

[24] W. Schabel, P. Scharfer, M. Kind, I. Mamaliga, Sorption and diffusion measurements in ternary polymer–solvent–solvent systems by means of a magnetic suspension balance—Experimental methods and correlations with a modified Flory–Huggins and free-volume theory, Chem. Eng. Sci. 62 (2007) 2254–2266. doi:10.1016/j.ces.2006.12.062.

[25] J.S. Vrentas, J.L. Duda, H.C. Ling, Enhancement of impurity removal from polymer films, J. Appl. Polym. Sci. 30 (1985) 4499–4516. doi:10.1002/app.1985.070301201.

[26] S. Alsoy, J.L. Duda, Modeling of multicomponent drying polymer films, AIChE J. 45 (1999) 896–905. doi:10.1002/aic.690450420.

[27] P.E. Price, I.H. Romdhane, Multicomponent diffusion theory and its applications to polymer-solvent systems, AIChE J. 49 (2003) 309–322. doi:10.1002/aic.690490204.

[28] V.K. Vanag, I.R. Epstein, Cross-diffusion and pattern formation in reaction-diffusion systems., Phys. Chem. Chem. Phys. 11 (2009) 897–912. doi:10.1039/b813825g.

[29] A.J. Cancelas, M.A. Plata, M.A. Bashir, M. Bartke, V. Monteil, T.F.L. McKenna, Solubility and Diffusivity of Propylene, Ethylene, and Propylene-Ethylene Mixtures in Polypropylene, Macromol. Chem. Phys. 219 (2018) 1700565. doi:10.1002/macp.201700565.

[30] S. Alsoy, J.L. Duda, Influence of swelling and diffusion-induced convection on polymer sorption processes, AIChE J. 48 (2002) 1849–1855. doi:10.1002/aic.690480903.

[31] V. Kanellopoulos, D. Mouratides, E. Tsiliopoulou, C. Kiparissides, An Experimental and Theoretical Investigation into the Diffusion of Olefins in Semi-Crystalline

Polymers: The Influence of Swelling in Polymer-Penetrant Systems, Macromol. React. Eng. 1 (2007) 106–118.

[32] M. Zhu, D. Vesely, The effect of polymer swelling and resistance to flow on solvent diffusion and permeability, Eur. Polym. J. 43 (2007) 4503–4515. doi:10.1016/J.EURPOLYMJ.2007.07.012.

[33] I.C. Sanchez, R.H. Lacombe, Statistical Thermodynamics of Fluid Mixtures, J. Phys. Chem. 80 (1976) 2568–2580.

[34] B. guo Wang, H. ling Lv, J. chu Yang, Estimation of solvent diffusion coefficient in amorphous polymers using the Sanchez-Lacombe equation-of-state, Chem. Eng. Sci. 62 (2007) 775–782. doi:10.1016/j.ces.2006.10.020.

[35] R. Simha, T. Somcynsky, On the Statistical Thermodynamics of Spherical and Chain Molecule Fluids, Macromolecules. 2 (1969) 342–350. doi:10.1021/ma60010a005.

[36] I.C. Sanchez, R.H. Lacombe, An elementary equation of state for polymer liquids, J. Polym. Sci. Polym. Lett. Ed. 15 (1977) 71–75. doi:10.1002/pol.1977.130150202.

[37] I.C. Sanchez, R.H. Lacombe, An elementary molecular theory of classical fluids. Pure fluids, J. Phys. Chem. 80 (1977) 2352–2362. doi:10.1021/j100562a008.

[38] M.A. Bashir, M. Al-haj Ali, V. Kanellopoulos, J. Seppälä, Modelling of multicomponent olefins solubility in polyolefins using Sanchez-Lacombe equation of state, Fluid Phase Equilib. 358 (2013) 83–90. doi:10.1016/j.fluid.2013.08.009.

[39] A. Alizadeh, Study of Sorption, Heat and Mass Transfer During Condensed Mode Operation of Gas Phase Ethylene Polymerization on Supported Catalyst, Queen's University, 2014.

[40] J.D. Ferry, Viscoelastic properties of polymers, Wiley, 1980.

[41] J.S. Vrentas, C.-H. Chu, M.C. Drake, E. von Meerwall, Predictive capabilities of a free-volume theory for solvent self-diffusion coefficients, J. Polym. Sci. Part B Polym. Phys. 27 (1989) 1179–1184. doi:10.1002/polb.1989.090270517.

[42] V. Kanellopoulos, M.A. Ali, S. Sundvall, S. Das, Experimental and Theoretical Study on the Desorption of Alcohols and Ketones from Polyolefins, Ind. Eng. Chem. Res. 52

(2013) 15855–15862. doi:10.1021/ie402479e.

[43] M. Tahmooresi, F. Sabzi, Methane Adsorption in a Series of IRMOFs Studied by PHSC and Sanchez–Lacombe Equations of State, J. Inorg. Organomet. Polym. Mater. 25 (2015) 1298–1304. doi:10.1007/s10904-015-0240-3.

[44] V. Kanellopoulos, D. Mouratides, P. Pladis, C. Kiparissides, Prediction of Solubility of α-olefins in Polyolefins Using a combined Equation of State - Molecular Dynamics Approach, Ind. Eng. Chem. Res. 45 (2006) 5870–5878.

[45] M.A. Bashir, M. Al-haj Ali, V. Kanellopoulos, J. Seppälä, E. Kokko, S. Vijay, The Effect of Pure Component Characteristic Parameters on Sanchez-Lacombe Equation-of-State Predictive Capabilities, Macromol. React. Eng. 7 (2013) 193–204. doi:10.1002/mren.201200054.

[46] W. Yao, X. Hu, Y. Yang, Modeling solubility of gases in semicrystalline polyethylene, J. Appl. Polym. Sci. 103 (2007) 1737–1744. doi:10.1002/app.24969.

[47] B. Flaconneche, J. Martin, M.H. Klopffer, Permeability, Diffusion and Solubility of Gases in Polyethylene, Polyamide 11 and Poly (Vinylidene Fluoride), Oil Gas Sci. Technol. 56 (2001) 261–278. doi:10.2516/ogst:2001023.

[48] J.E. Mark, Physical properties of polymer handbook, Springer, 2006.

[49] A. Gonzalez, S. Eceolaza, A. Etxeberria, J.J. Iruin, Diffusivity of ethylene and propylene in atactic and isotactic polypropylene: Morphology effects and free-volume simulations, J. Appl. Polym. Sci. 104 (2007) 3871–3878. doi:10.1002/app.26000.

[50] D.R. Sturm, Diffusivity and Solubility of Solvents in Semi-crystalline and Glassu Polymers, The Pennsylvania State University, 2017. https://etda.libraries.psu.edu/catalog/14133dxs84 (accessed January 22, 2019).

[51] D.J. Plazek, K.L. Ngai, The Glass Temperature, in: Phys. Prop. Polym. Handb., Springer New York, New York, NY, 2007: pp. 187–215. doi:10.1007/978-0-387-69002-5_12.

[52] J. Crank, The mathematics of diffusion, Clarendon Press, 1975. https://books.google.fr/books/about/The_Mathematics_of_Diffusion.html?id=eHANhZwVouYC&hl=fr (accessed March 27, 2019).